Available online at www.sciencedirect.com
SCIENCE DIRECT
Journal of Organometallic Chemistry 691 (2006) 3545–3555
Journal of Organometallic Chemistry
www.elsevier.com/locate/jorganchem

Half-sandwich η^6-benzene Ru(II) complexes of pyridylpyrazole and pyridylimidazole ligands: Synthesis, spectra, and structure

Haritosh Mishra, Rabindranath Mukherjee *

Department of Chemistry, Indian Institute of Technology Kanpur, Kanpur 208 016, India

Received 10 March 2006; received in revised form 25 April 2006; accepted 27 April 2006
Available online 5 May 2006

Abstract

New series of half-sandwich ruthenium(II) complexes supported by a group of bidentate pyridylpyrazole and pyridylimidazole ligands $[(\eta^6\text{-}C_6H_6)Ru(L^2)Cl][PF_6]$ (**1**), $[(\eta^6\text{-}C_6H_6)Ru(HL^3)Cl][PF_6]$ (**2**), $[(\eta^6\text{-}C_6H_6)Ru(L^4)Cl][PF_6]$ (**3**), and $[(\eta^6\text{-}C_6H_6)Ru(HL^5)Cl][PF_6]$ (**4**) [L^2, 2-[3-(4-chlorophenyl)pyrazol-1-ylmethyl]pyridine; HL^3, 3-(2-pyridyl)pyrazole; L^4, 1-benzyl-[3-(2′-pyridyl)]pyrazole; HL^5, 2-(1-imidazol-2-yl)pyridine] are reported. The molecular structures of **1**–**4** both in the solid state by X-ray crystallography and in solution using ^1H NMR spectroscopy have been elucidated. Further, the crystal packing in the complexes is stabilized by C–H···X (X = Cl and π), N–H···Cl, and π–π interactions.

Keywords: Ruthenium(II); Benzene; Pyridyl/pyrazole/imidazole ligands; Crystal structures; Non-covalent interactions

1. Introduction

Arene ruthenium compounds belong to a well-established family of robust metal-organic molecules that played an important role in the development of organometallic chemistry [1]. Continued interest in such systems arises due to their catalytic potential in a wide range of organic reactions [2,3] and very promising anticancer activity of $[(\eta^6\text{-arene})Ru(en)Cl]^+$ (en = 1,2-diaminoethane) class of complexes [4,5]. These findings provide the impetus for the synthesis and properties of new $\{(\eta^6\text{-}C_6H_6)Ru(L)\text{-}Cl\}^+$(L = bidentate N-donor ligand) complexes. Properties of the complexes are determined in large measure by the nature of ligands bound to the metal ion. For the complexes of pertinence to this study the role of a chelating ligand is to fine-tune the Ru–benzene bonding interaction. Although several examples of structurally characterized mononuclear three-legged half-sandwich organometallic complexes having $\{(\eta^6\text{-}C_6H_6)Ru\}^{2+}$ unit supported by N-donor ligands are known [6], there is no report in the literature, to our knowledge, of structurally characterized complexes of pyridyl/pyrazole/imidazole-hybrid chelating ligand systems containing two different heterocyclic N-donor sites in a given bidentate ligand. From the standpoint of synthetic chemistry we find it really challenging and in this report we provide examples of such structural motifs. In this study we have selected a uniformly varied group of bidentate heterocyclic N-donor ligands. They include: (i) a nonplanar pyridyl and a pyrazole unit of L^2 separated by a CH_2 spacer with a *p*-chlorophenyl ring directly attached to the pyrazole moiety; (ii) a planar directly attached pyridyl and pyrazole unit of HL^3; (iii) a planar directly attached pyridyl and pyrazole unit with the pyrazole moiety having an appended benzyl group of L^4; and (iv) a planar directly attached pyridyl and imidazole unit of HL^5. Notably, the two heterocyclic rings of the ligands HL^3, L^4, and HL^5 can communicate electronically; however, in the ligand L^2 such a situation does not exist.

The purpose of the present work is two-fold. First, during our investigations into the chemistry of three-legged

* Corresponding author. Tel.:/fax: +91 512 2597437/7436.
E-mail address: rnm@iitk.ac.in (R. Mukherjee).

0022-328X/$ - see front matter © 2006 Elsevier B.V. All rights reserved.
doi:10.1016/j.jorganchem.2006.04.037

"piano-stool" complexes [7] we prepared the complexes $[(\eta^6\text{-}C_6H_6)Ru(L^1)Cl][PF_6]$ [L^1 = 2-(pyrazol-1-ylmethyl) pyridine and its 3,5-dimethylpyrazole derivatives] [7a]. In an attempt to widen this class of half-sandwich ruthenium(II) complexes of "piano-stool geometry" we have investigated the reactions of the dimer $[\{(\eta^6\text{-}C_6H_6)RuCl(\mu\text{-}Cl)\}_2]$ with L^2, HL^3, L^4, and HL^5 and characterized the complexes $[(\eta^6\text{-}C_6H_6)Ru(L^2)Cl][PF_6]$ (**1**), $[(\eta^6\text{-}C_6H_6)Ru(HL^3)Cl][PF_6]$ (**2**), $[(\eta^6\text{-}C_6H_6)Ru(L^4)Cl][PF_6]$ (**3**), and $[(\eta^6\text{-}C_6H_6)Ru(HL^5)Cl][PF_6]$ (**4**). We wished to test if the different electronic/steric environment provided by a particular bidentate ligand has an impact on the relative strength of Ru–benzene bonding.

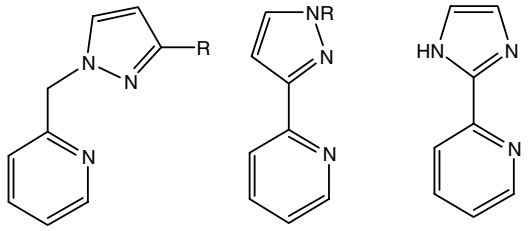

R = H (L^1) = -C_6H_4-*p*-Cl (L^2) R = H (HL^3) = -CH_2-C_6H_5 (L^4) HL^5

Secondly, existence of non-covalent interactions [8,9] and particularly C–H···Cl interactions [10–13] have been identified in organometallic molecules, including half-sandwich complexes $[(\eta^6\text{-}C_6H_6)Ru(L)Cl]^+$ (L = two monodentate or a bidentate neutral N-donor ligand) [5a,6k], $[(\eta^6\text{-}C_6H_6)Ru(Me_2HPz)Cl_2]$ [6k], and $[(\eta^6\text{-}C_6H_6)Ru(L)(PPh_3)Cl]^+$ (L = 1-(4-cyanophenyl)imidazole) [11d]. From this background and our own activity in this field [14] we wished to identify primarily C–H···Cl hydrogen-bonding interactions in the present group of half-sandwich "piano-stool" organometallic molecules. In this report we investigate the use of the half-sandwich organometallic units $\{(\eta^6\text{-}C_6H_6)Ru(L)Cl\}^+$ present in **1**–**4** to demonstrate a rich variety of non-covalent (C–H···Cl–Ru, N–H···Cl–Ru hydrogen-bonding; C–H···π and π–π) interactions.

2. Experimental

2.1. Materials

Reagent or analytical grade starting materials were obtained from commercial suppliers and used without further purification. The ligands 3-(2-pyridyl)pyrazole (HL^3) [15], 1-benzyl-[3-(2′-pyridyl)pyrazole (L^4) [16], and 2-(1-imidazol-2-yl)pyridine (HL^5) [17] were synthesized following the literature procedures. The dimer $[\{(\eta^6\text{-}C_6H_6)RuCl(\mu\text{-}Cl)\}_2]$ was prepared following a reported procedure [18].

2.2. Preparation of ligand

2.2.1. 2-[3-(4-Chlorophenyl)pyrazol-1-ylmethyl]pyridine (L^2)

The starting material 3-(4-chlorophenyl)-1-pyrazole necessary for the synthesis of L^2 was prepared following a procedure similar to that used for the synthesis of HL^3 [15]. A solution of 1-(4-chlorophenyl)ethanone (2.0 g, 0.013 mol) in *N*,*N*-dimethylformamide dimethylacetal (5 mL; 4.7 g, 0.039 mol) was refluxed for 10 h. After cooling to 25 °C, the excess of solvent was removed under reduced pressure. The resulting sticky solid was dried in vacuo and used in next step without further purification. Yield: 1.64 g, ca. 70%. A mixture of resulting compound 1-(4-chlorophenyl)but-2-en-1-one (1.64 g, 0.009 mol) and hydrazine hydrate (4 mL) in EtOH (3 mL) was stirred at 60 °C for 30 min. After cooling to 25 °C, the reaction mixture was poured into 20 g of ice which afforded a white precipitate. It was filtered, washed with cold water several times and dried in air. Recrystallization from chloroform/*n*-hexane mixture afforded a white crystalline solid. Yield: 1.04 g, ca. 65%. ^{1}H NMR (80 MHz; $CDCl_3$): 6.32 (1H, d, pyrazole H_4), 7.30–7.58 (4H, m, benzene), 7.65 (1H, d, pyrazole H_5).

A mixture of 2-(chloromethyl)pyridine hydrochloride (0.92 g, 5.62 mmol), 3-(4-chlorophenyl)-1-pyrazole (1.0 g, 5.62 mmol), benzene (60 mL), 40% aqueous NaOH (8 mL), and 40% aqueous tetra-*n*-butylammonium hydroxide (8 drops) was refluxed with stirring for 8 h and then stirred at 25 °C for 12 h. The organic layer was then separated, washed twice with brine water (100 mL), dried over anhydrous $MgSO_4$, and filtered. Solvent removal afforded a thick yellowish white solid. Yield: 1.06 g, ca. 70%. The ligand was further purified by recrystallization from chloroform/*n*-hexane. ^{1}H NMR (80 MHz; $CDCl_3$): δ 5.42 (2H, s, CH_2), 6.54 (1H, d, pyrazole H_4), 7.00–7.68 (7H, m, pyridine $H_{3,4,5}$ and phenyl $H_{2,3,5,6}$), 7.80 (1H, d, pyrazole H_5), 8.62 (1H, d, pyridine H_6).

2.3. Preparation of complexes

2.3.1. General procedure

The ligand (0.4 mmol) was dissolved in MeOH (15 mL) and to it was added solid $[\{(\eta^6\text{-}C_6H_6)RuCl(\mu\text{-}Cl)\}_2]$ (0.2 mmol). The mixture was stirred for 12 h (complexes **1**, **2**, and **3**) or 6 h (complex **4**) at 25 °C. The resulting yellow (complexes **1**, **2**, and **4**) or orange (complex **3**) solution was filtered and the volume of the filtrate was reduced (7 mL), and to it was added solid NH_4PF_6 (0.4 mmol). The yellow or orange microcrystalline solid that formed was filtered, washed with cold MeOH, and dried in vacuo. Recrystallization was achieved from hot MeOH solutions. X-ray quality single crystals were obtained by diffusion of diethyl ether into a solution (1 mL) of the compound in a mixture of MeOH and MeCN (v/v, 1:4 for complex **1**; v/v, 1:2 for complex **3**; v/v, 1:1 for complex **4**) or in MeCN (complex **2**).

*2.3.2. [(η^6-C_6H_6)Ru(L^2)Cl][PF_6] (**1**)*

Yield: 0.125 g, 49.7%. Anal. Calc. $C_{21}H_{18}Cl_2F_6N_3PRu$: C, 40.06; H, 2.86; N, 6.67. Found: C, 40.14; H, 2.84; N, 6.69%. ^{1}H NMR (CD_3CN; 400 MHz; 25 °C): δ 9.06 (d, $J_{HH} = 5.8$ Hz, 1H, H_6 of py), 8.05 (d, $J_{HH} = 8.3$ Hz, 1H, $H_{5'}$ of pz), 7.99 (t, $J_{HH} = 8.0$ Hz, 1H, H_4 of py), 7.72 (m, 3H, H_5 of py, $H_{3''}$, $H_{4''}$ of phenyl), 7.56 (m, 3H, H_3 of py and $H_{2''}$, $H_{5''}$ of phenyl), 6.56 (d, $J_{HH} = 7.1$ Hz, 1H, $H_{4'}$ of pz), 5.72 (s, 6H, C_6H_6), 5.72 (1H, CH_2–, overlaps with C_6H_6 resonance), 5.44 (d, $J_{gem} = 9.8$ Hz, 1H, CH_2–). Molar conductance, Λ_M (MeCN, 25 °C) = 145 Ω^{-1} cm^2 mol^{-1} (expected 1:1 range: 120–160 Ω^{-1} cm^2 mol^{-1}) [19]. UV–VIS (in MeCN): λ/nm (ε/dm^3 mol^{-1} cm^{-1}) 230 (24900), 412 (450). IR (KBr, cm^{-1}): 838 $\nu(PF_6^-)$.

*2.3.3. [(η^6-C_6H_6)Ru(HL^3)Cl][PF_6] (**2**)*

Yield: 0.135 g, 66.9%. Anal. Calc. $C_{14}H_{13}ClF_6N_3PRu$: C, 33.29; H, 2.58; N, 8.32. Found: C, 33.43; H, 2.62; N, 8.46%. IR (KBr, cm^{-1}): 838 $\nu(PF_6^-)$. Molar conductance, Λ_M (MeCN, 25 °C) = 140 Ω^{-1} cm^2 mol^{-1}. ^{1}H NMR (CD_3CN; 400 MHz; 298 K): δ 9.32 (d, $J_{HH} = 5.6$ Hz, 1H, H_6 of py), 8.09–7.98 (m, 3H, H_3 and H_4 of py and $H_{5'}$ of pz), 7.53 (dd, $J^1_{HH} = 7.1$ Hz, $J^2_{HH} = 6.1$ Hz, 1H, H_5 of py), 7.02 (d, $J_{HH} = 2.7$ Hz, 1H, $H_{4'}$ of pz), 6.02 (s, 6H, C_6H_6). UV–VIS (in MeCN): λ/nm (ε/dm^3 mol^{-1} cm^{-1}) 260 sh (8350), 292 (10000), 320 sh (4400), 407 (600).

*2.3.4. [(η^6-C_6H_6)Ru(L^4)Cl][PF_6] (**3**)*

Yield: 0.100 g, 56.1%. Anal. Calc. $C_{21}H_{19}ClF_6N_3PRu$: C, 42.42; H, 3.20; N, 7.07. Found: C, 42.45; H, 3.18; N, 7.12%. IR (KBr, cm^{-1}): 841 $\nu(PF_6^-)$. Molar conductance, Λ_M (MeCN, 25 °C) = 115 Ω^{-1} cm^2 mol^{-1}. ^{1}H NMR (CD_3CN; 400 MHz; 25 °C): δ 9.28 (d, $J_{HH} = 5.6$ Hz, 1H, H_6 of py), 8.09 (t, $J_{HH} = 7.8$ Hz, 1H, H_4 of py), 7.95 (d, $J_{HH} = 7.8$ Hz, 1H, $H_{5'}$ of pz), 7.70 (d, $J_{HH} = 2.9$ Hz, 1H, H_3 of py), 7.57 (t, $J_{HH} = 5.8$ Hz, 1H, H_5 of py), 7.38–7.50 (5H, $H_{2''-6''}$ of benzyl), 7.03 (d, $J_{HH} = 2.7$ Hz, 1H, $H_{4'}$ of pz), 6.01 (s, 6H, C_6H_6), 5.87 (d, $J_{gem} = 15.9$ Hz, 1H, NCH_2–), 5.74 (d, $J_{gem} = 15.2$ Hz, 1H, NCH_2–). UV–VIS (in MeCN): λ/nm (ε/dm^3 mol^{-1} cm^{-1}) 260 (12150), 300 (13450), 415 (550).

*2.3.5. [(η^6-C_6H_6)Ru(HL^5)Cl][PF_6] (**4**)*

Yield: 0.135 g, 66.9%. Anal. Calc. $C_{14}H_{13}ClF_6N_3PRu$: C, 33.29; H, 2.58; N, 8.32. Found: C, 33.43; H, 2.62; N, 8.46%. IR (KBr, cm^{-1}): 838 $\nu(PF_6^-)$. Molar conductance, Λ_M (MeCN, 298 K) = 120 Ω^{-1} cm^2 mol^{-1}. ^{1}H NMR (CD_3CN; 400 MHz; 25 °C): δ 9.32 (d, $J_{HH} = 4.4$ Hz, 1H, H_6 of py), 8.94 (d, $J_{HH} = 6.6$ Hz, 1H, $H_{4'}$ of HIm), 7.93 (d, $J_{HH} = 7.1$ Hz, 1H, $H_{5'}$ of HIm), 7.67 (t, $J_{HH} = 2.5$ Hz, 1H, H_4 of py), 7.54 (t, $J_{HH} = 2.6$ Hz, 1H, H_5 of py), 7.45 (t, $J_{HH} = 4.2$ Hz, 1H, H_3 of py), 5.94 (s, 6H, C_6H_6). UV–VIS (in MeCN): λ/nm (ε/dm^3 mol^{-1} cm^{-1}) 270 sh (11200), 304 (13450), 400 (650).

2.4. Instrumentation

Elemental analyses were obtained using Thermo Quest EA 1110 CHNS-O, Italy. Conductivity measurements were done with an Elico type CM-82T conductivity bridge (Hyderabad, India). Spectroscopic measurements were made using the following instruments: IR (KBr, 4000–600 cm^{-1}), Bruker Vector 22; electronic, Perkin–Elmer Lambda 2 and Agilent 8453 diode-array spectrophotometer. ^{1}H NMR spectral measurements were performed on a JEOL-JNM-LA-400 FT (400 MHz) NMR spectrometer.

2.5. Crystal structure determination

Diffraction intensities were collected on a Bruker SMART APEX CCD diffractometer at 100(2) K using graphite-monochromated Mo Kα ($\lambda = 0.710\ 69$ Å) radiation. Intensity data were corrected for Lorentz polarization effects. Empirical absorption correction (SADABS) was applied. The structures were solved by SIR-97, expanded by Fourier-difference syntheses and refined with SHELXL-97, incorporated in WINGX 1.64 crystallographic collective package [20]. Hydrogen atoms were placed in idealized positions, and treated using riding model approximation with displacement parameters derived from those of the atoms to which they were bonded. All non-hydrogen atoms were refined with anisotropic thermal parameters by full-matrix least-squares procedures on F^2. A summary of the data collection and structure refinement information is provided in Table 1. Intermolecular contacts of the C–H···Cl, N–H···Cl, π–π types and an intramolecular contact of the C–H···π type were examined with the DIAMOND package [21]. C–H and N–H distances were normalized along the same vectors to the neutron derived values of 1.083 Å and 1.009 Å, respectively [12c].

3. Results and discussion

3.1. Synthesis and characterization of complexes

Reactions of chloro-bridged dimer [{(η^6-C_6H_6)RuCl(μ-Cl)}$_2$] with L^2, HL^3, L^4, and HL^5 in MeOH followed by subsequent treatment with NH_4PF_6 resulted in the isolation of [(η^6-C_6H_6)Ru(L^2)Cl][PF_6] (**1**), [(η^6-C_6H_6)Ru(HL^3)Cl][PF_6] (**2**), [(η^6-C_6H_6)Ru(L^4)Cl][PF_6] (**3**), and [(η^6-C_6H_6)Ru(HL^5)Cl][PF_6] (**4**), as microcrystalline solid. The synthesis of compounds **1**–**4** passes through chloro bridge-cleavage reactions of [{(η^6-C_6H_6)RuCl(μ-Cl)}$_2$].

Characterization of the new compounds was accomplished by elemental analysis, solution electrical conductivity, IR, and ^{1}H NMR spectroscopy. Consistent with their formulation, conductivity studies revealed that compounds **1**–**4** are 1:1 electrolyte [19]. As proof of their yellow to yellow orange color, compounds **1**–**4** exhibit absorption spectral band in the 400–415 nm region, due to $Cl^- \rightarrow Ru(II)$ charge-transfer transition.

Table 1
Data collection and structure refinement parameters for $[(\eta^6\text{-}C_6H_6)Ru(L^2)Cl][PF_6]$ (**1**), $[(\eta^6\text{-}C_6H_6)Ru(HL^3)Cl][PF_6]$ (**2**), $[(\eta^6\text{-}C_6H_6)Ru(L^4)Cl][PF_6]$ (**3**), and $[(\eta^6\text{-}C_6H_6)Ru(HL^5)Cl][PF_6]$ (**4**)

	1	**2**	**3**	**4**
Chemical formula	$C_{21}H_{18}N_3Cl_2PF_6Ru$	$C_{14}H_{13}N_3ClPF_6Ru$	$C_{21}H_{19}N_3ClPF_6Ru$	$C_{14}H_{13}N_3ClPF_6Ru$
M	629.32	504.76	594.88	504.76
Crystal colour, habit	Yellow, block	Orange, block	Orange, block	Orange, block
T (K)	100(2)	100(2)	100(2)	100(2)
Crystal system	Triclinic	Monoclinic	Triclinic	Monoclinic
Space group	$P\bar{1}$ (#2)	$P2_1/c$ (#14)	$P\bar{1}$ (#2)	$P2_1/n$ (#14)
a (Å)	12.693(5)	7.206(5)	9.329(5)	7.785(5)
b (Å)	12.784(5)	21.640(5)	10.208(5)	8.385(5)
c (Å)	15.506(5)	10.803(5)	11.917(5)	25.934(5)
α (°)	79.616(5)	90.0	108.051(5)	90.0
β (°)	72.429(5)	102.110(5)	94.686(5)	92.326(5)
γ (°)	69.404(5)	90.0	93.945(5)	90.0
V (Å)^3	2238.0(14)	1647.1(14)	1070.1(9)	1691.5(15)
Z	4	4	2	4
d_{calc} (g cm^{-3})	1.868	2.036	1.846	1.982
μ/mm^{-1}	1.077	1.279	1.000	1.245
$F(000)$	1248	992	592	992
Number of reflections collected	14924	10996	7082	10977
Number of independent reflections [R_{int}]	10495 [0.0192]	4069 [0.0239]	5014 [0.0155]	4186 [0.0485]
Number of reflections used [$I > 2\sigma(I)$]	8924	3838	4590	3487
GOF on F^2	1.119	1.074	1.272	1.142
Final R indices [$I > 2\sigma(I)$][a,b]	0.0450, 0.1060	0.0241, 0.0583	0.0351, 0.0756	0.0688, 0.1436
Final R indices (all data)	0.0549, 0.1154	0.0262, 0.0595	0.0466, 0.1086	0.0855, 0.1540

[a] $R_1 = \sum(|F_o| - |F_c|)/\sum|F_o|$.
[b] $wR_2 = \{\sum[w(|F_o|^2 - |F_c|^2)^2]/\sum[w(|F_o|^2)^2]\}^{1/2}$.

3.2. Molecular structures of $[(\eta^6\text{-}C_6H_6)Ru(L^2)Cl][PF_6]$ (**1**), $[(\eta^6\text{-}C_6H_6)Ru(HL^3)Cl][PF_6]$ (**2**), $[(\eta^6\text{-}C_6H_6)Ru(L^4)Cl][PF_6]$ (**3**), and $[(\eta^6\text{-}C_6H_6)Ru(HL^5)Cl][PF_6]$ (**4**)

In order to confirm the identity of the chloride-bound structures of the cations in **1**–**4** crystal structure analyses were undertaken. Structural analysis of **1** revealed that the asymmetric unit contains two crystallographically independent molecules. Both molecules have essentially identical coordination geometry, but the corresponding bond lengths and bond angles are slightly different. The data for the molecule, which is not shown, are in brackets (Table 2). X-ray crystallographic analyses confirm the structures

Table 2
Selected bond lengths (Å) and angles (°) in $[(\eta^6\text{-}C_6H_6)Ru(L^2)Cl][PF_6]$ (**1**), $[(\eta^6\text{-}C_6H_6)Ru(HL^3)Cl][PF_6]$ (**2**), $[(\eta^6\text{-}C_6H_6)Ru(L^4)Cl][PF_6]$ (**3**), and $[(\eta^6\text{-}C_6H_6)Ru(HL^5)Cl]\text{-}[PF_6]$ (**4**)

	1[a]	**2**	**3**	**4**
Ru(1)–N(1)	2.117(4) [2.121(4)]	2.1095(17)	2.118(4)	2.123(5)
Ru(1)–N(3)	2.111(4) [2.109(4)]	2.0511(17)	2.107(3)	2.072(5)
Ru(1)–Cl(1)	2.4000(12) [2.3968(12)]	2.4170(13)	2.4155(13)	2.4249(16)
Ru(1)–C(1)	2.182(4) [2.177(4)]	2.200(2)	2.191(4)	2.195(8)
Ru(1)–C(2)	2.195(4) [2.215(4)]	2.186(2)	2.184(4)	2.180(7)
Ru(1)–C(3)	2.190(4) [2.176(4)]	2.168(2)	2.200(4)	2.167(6)
Ru(1)–C(4)	2.199(4) [2.200(4)]	2.175(2)	2.190(4)	2.176(6)
Ru(1)–C(5)	2.194(4) [2.185(5)]	2.165(2)	2.192(4)	2.151(7)
Ru(1)–C(6)	2.194(4) [2.191(4)]	2.213(2)	2.188(4)	2.193(7)
C(1)–C(2)	1.399(6) [1.408(6)]	1.415(3)	1.392(6)	1.429(11)
C(2)–C(3)	1.424(6) [1.427(6)]	1.410(3)	1.432(6)	1.403(11)
C(3)–C(4)	1.400(6) [1.407(7)]	1.422(3)	1.394(6)	1.415(11)
C(4)–C(5)	1.424(6) [1.406(7)]	1.409(3)	1.422(6)	1.401(11)
C(5)–C(6)	1.396(6) [1.400(6)]	1.427(3)	1.406(6)	1.403(13)
C(1)–C(6)	1.427(6) [1.424(6)]	1.396(3)	1.421(6)	1.385(12)
N(1)–Ru–N(3)	84.70(16) [83.85(15)]	75.62(7)	75.83(14)	76.3(2)
N(1)–Ru–Cl(1)	82.66(11) [84.71(11)]	85.51(6)	86.44(11)	85.87(14)
N(3)–Ru–Cl(1)	88.44(11) [86.49(11)]	83.90(6)	84.39(9)	85.31(14)

[a] The data are for two molecules.

of the compounds **1**–**4** (Figs. 1 and 2, Table 2). The cations exhibit the expected and usual pseudo-octahedral half-sandwich "piano-stool" disposition around the Ru atom [6,7a], with the benzene ligand occupying one face of the octahedron (the ruthenium atom is π bonded to the η^6-C_6H_6 group) and the coordination of a bidentate heterocyclic N-donor ligand [N(1) of pyridyl ring and N(3) of other heterocyclic ring of pyrazole/imidazole] and a chloride ion on the other face. The N–Ru–N angles have values of 84.70(16)° [83.85(15)°] (**1**), 75.62(7)° (**2**), 75.83(14)° (**3**), and 76.3(2)° (**4**), deviated from 90° as per demand of the bite of the ligand. The bite angle is ~76° when two heterocyclic units, a six-membered and a five-membered, are directly attached and the angle is in the range 83–85°, when the two rings are separated by a methylene spacer.

In the case of **1** the pyridyl and pyrazole rings of L^2 are each planar; however, the pyridyl mean plane is tilted to adjacent pyrazole ring at an angle of 51.62(7)° [61.68(7)°], attesting its nonplanarity [22,23]. In addition, the pyrazole ring and *p*-chlorophenyl group in L^2 make an angle of 76.86(12)° [63.93(12)°]. The pyridyl and pyrazole/imidazole rings of HL^3 in **2** or of L^4 in **3** or of HL^5 in **4** are each planar and also planar to each other [the angle between the two heterocyclic rings: 3.60(11)° (**2**); 10.61(15)° (**3**) (the pyrazole ring and phenyl group make an angle of 89.47(15)°); 1.64(6)° for (**4**)].

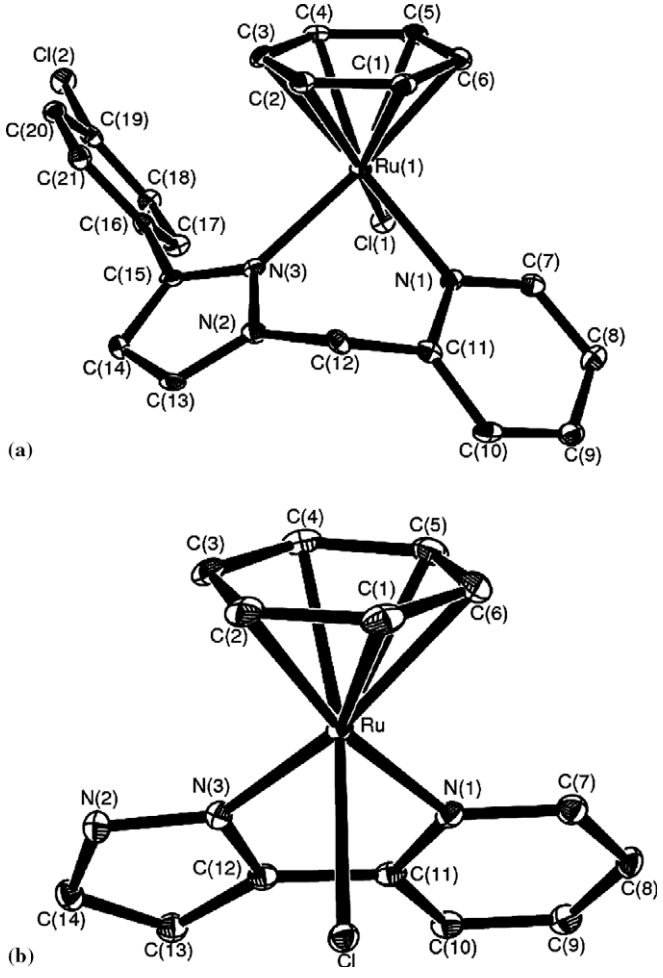

Fig. 1. Thermal ellipsoid plots of: (a) $[(\eta^6\text{-}C_6H_6)Ru(L^2)Cl]^+$ in **2** and (b) $[(\eta^6\text{-}C_6H_6)Ru(HL^3)Cl]^+$ in **3** at 30% probability level. Hydrogen atoms have been omitted for clarity.

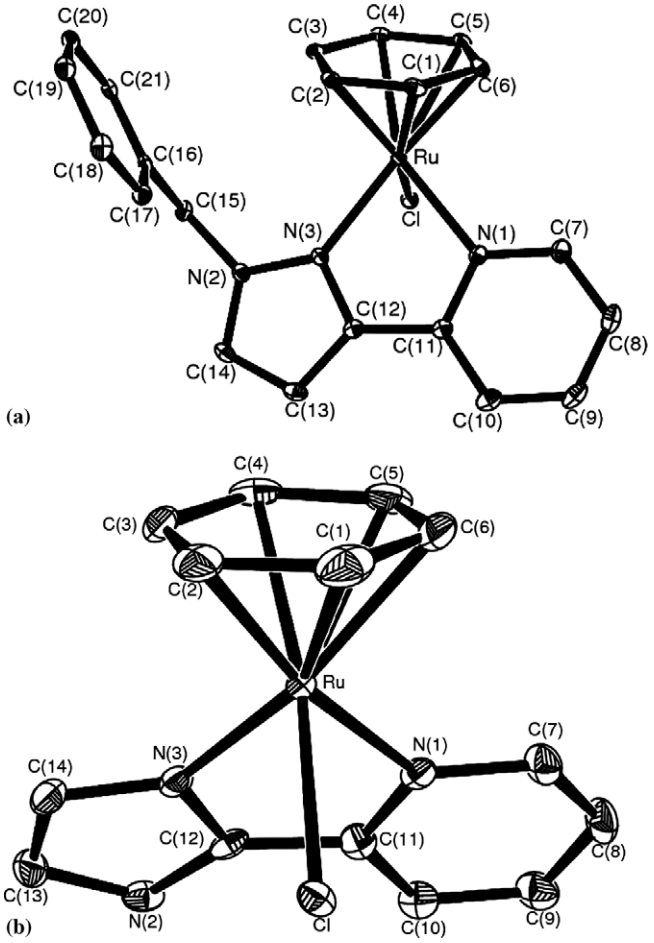

Fig. 2. Thermal ellipsoid plots of: (a) $[(\eta^6\text{-}C_6H_6)Ru(L^4)Cl]^+$ in **3** and (b) $[(\eta^6\text{-}C_6H_6)Ru(HL^5)Cl]^+$ in **4** at 30% probability level. Hydrogen atoms have been omitted for clarity.

For complexes **1**–**4** the observed trend in Ru–C, Ru–N(py), Ru–N(pz), Ru–N(im) or Ru–Cl distances, reflecting mutual *trans* influence, is a consequence of interplay between steric and electronic factors associated with the coordinating ability of bidentate ligands L^2, HL^3, L^4 or HL^5, in a closely similar metal coordination environment.

Interestingly, X-ray structural analyses revealed noticeable differences in the bonding characteristics (metric parameters) of bidentate ligands L^2, HL^3, L^4 and HL^5 as well as the characteristics of π-bonded benzene rings in these cations (Tables 2 and 3). From a careful look at the metric parameters of Table 3, which lists pertinent bonding parameters for the complexes **1**–**4**, the following generalizations emerge. (i) Within the complexes **1**–**3**, the pyrazole binds stronger than pyridine and the pyrazole ring directly attached to pyridine (HL^3 and L^4) binds stronger than the pyrazole ring attached to pyridine with a methylene spacer (L^2). (ii) Between the complexes **2** and **3**, the presence of

Table 3
Summary of relevant bond distances (Å) in $[(\eta^6\text{-}C_6H_6)Ru(L^2)Cl][PF_6]$ (**1**), $[(\eta^6\text{-}C_6H_6)Ru(HL^3)Cl][PF_6]$ (**2**), $[(\eta^6\text{-}C_6H_6)Ru(L^4)Cl][PF_6]$ (**3**), and $[(\eta^6\text{-}C_6H_6)Ru(HL^5)Cl]\text{-}[PF_6]$ (**4**)

	1[a]	**2**	**3**	**4**
Av Ru–C	2.192(4) [2.190 (4)][a]	2.184(2)	2.190(4)	2.177(7)
Ru–C_6H_6 centroid	1.677 (1.675)[a]	1.666	1.676	1.662
Av C–C	1.411(7) [1.412(7)][a]	1.413(3)	1.411(6)	1.406(12)
Ru–N(py)	2.117(4) [2.121(4)][a]	2.1095(17)	2.118(4)	2.123(5)
Ru–N(Im)	–	–	–	2.072(5)
Ru–N(pz)	2.111(4) [2.109(4)][a]	2.0511(17)	2.107(3)	–
Ru–Cl	2.4000(12) [2.3968(12)][a]	2.4170(13)	2.415(13)	2.4249(16)

[a] The data are for two molecules.

steric effect is revealed in L^4 over HL^3. (iii) Between the complexes **2** and **4**, pyrazole (HL^3) binds stronger than imidazole (HL^5). (iv) Within the present group of complexes **1**–**4**, both pyridine and pyrazole in the ligand HL^3 bind most effectively in **2** and the least effective binding of pyridine and pyrazole are observed by the ligands L^4 and L^2, respectively.

The Ru–N(py) and Ru–N(pz) distances in **2** are uniformly shorter than those in **1** by ~0.007 Å and ~0.06 Å, respectively (Table 3). Thus the pyrazole ring of HL^3 binds strongly to ruthenium(II) in **2** compared to that of pyrazole ring of L^2 in **1**. This trend must be associated with the planarity of HL^3 for a better metal-ligand orbital overlap than that in the case with nonplanar L^2. A general trend of pyrazole coordinating better than pyridine, as observed in **1**–**3** was observed before in *trans*-$[Co(L^1)_2Cl_2]$ [23], $[Zn(L^1)Cl_2]$ [14a], $[Fe_2(HL^3)_4(\mu\text{-}O)(OSO_3)_2]\cdot 2MeOH\cdot 3H_2O$ [24], $[Cu(L^4)(MeCN)_2][ClO_4]$ [16], and $[\{Cu(L^4)(dmf)(\mu\text{-}O_2C\text{-}Me)\}_2][ClO_4]_2\cdot dmf\cdot 0.5MeCO_2H$ [16]. In **4** the observed trend of imidazole binding Ru(II) stronger than pyridine follows a similar trend. The shortest Ru–C_6H_6 centroid distance in **2** clearly reveals that amongst pyridylpyrazole ligands present in **1**–**3** the ligand HL^3 provides maximum relative strength of $\{(\eta^6\text{-}C_6H_6)Ru\}^{2+}$ unit.

Average Ru–C distances in **1**–**4** (Table 3) are comparable to that reported in similar three-legged piano-stool complexes including $\{(\eta^6\text{-}C_6H_6)RuCl\}^+$ moiety [6,7a]. The Ru–N(py) bond lengths observed in **1**–**4** and Ru–N(pz) bond lengths observed in **1**–**3** compare well with the values found in similar three-legged piano-stool complexes including $\{(\eta^6\text{-}C_6H_6)RuCl\}^+$ moiety, with N-donor ligands [6a,6i,6k,7a]. The Ru-Cl distances are comparable to that reported in the literature for closely similar complexes [6f,6i,6k,6l,25].

3.3. ^1H NMR spectroscopy

^1H NMR spectroscopy provides easy means of characterization of these half-sandwich compounds. The data (in CD_3CN) along with their assignments are recorded in Section 2, supporting their expected "piano-stool" structure. The spectral feature of compounds **1**–**4** displayed in Figs. S1–S4 (Supplementary material) is consistent with the presence of a coordinated benzene ligand and a bidentate ligand L^1, L^2, HL^3, L^4 or HL^5. The proton resonances were assigned based on the available ^1H NMR spectral results for the free ligands L^2 (this work), HL^3 [15], L^4 [16], and HL^5 [17] and those for closely similar compounds [7a]. The following comments regarding the spectral data are in order. (i) The chemical shift values for coordinated benzene in chloro complexes **1**, **2**, **3**, and **4** are δ 5.72, δ 6.02, δ 6.01 and δ 5.94, respectively. Maximum upfield shift (δ 5.72) for **1** implies the presence of more electron density on the benzene ring. It is clearly reflected in its av Ru-C distance (Table 3), implying poor interaction of C_6H_6 ligand with Ru(II) (*cf.* X-ray structure). In the case of $[(\eta^6\text{-}C_6H_6)Ru(Me_2Hpz)Cl_2]$ (Me_2Hpz = 3,5-dimethylpyrazole) a similar high field (δ 5.76) shift of coordinated benzene was reported [6k]. For $[(\eta^6\text{-}C_6H_6)Ru(L^1)Cl][PF_6]$ the chemical shift value of δ 5.94 [7a], corroborates better coordination of C_6H_6 ligand than that in **1**. An AB quartet for CH_2 protons of L^2 in **1** confirms the presence of two diastereotopic protons, axial and equatorial. It implies that these protons are not interconverting on the NMR time-scale, otherwise a singlet would have resulted.

In essence, the ^1H NMR results of **1**–**4** clearly indicates that the solid state structures (vide supra) are retained in solution.

3.4. Non-covalent interactions

A closer inspection of the crystal packing diagrams of **1**–**4** reveals that these organometallic molecules are engaged in a number of secondary interactions (see below). Relevant bond distances, bond angles, and symmetry are summarized in Table 4. The C–H···Cl hydrogen-bonding parameters observed in this work [2.588–2.712 Å and 137.2–152.8° (**1**); 2.715 Å and 127.9° (**2**); 2.718–2.731 Å and 147.7–162.2° (**3**); 2.414 Å and 169.2°(**4**)] are in good agreement with literature tabulations (C–H···Cl: 2.569–2.944 Å and 119.3–169.2°) [10a], literature precedents [5a,6k,10–13] including our own findings [14]. These can be classified as intermediate contacts (2.41–2.73 Å), which are appreciably shorter than the sum of the van der Waals radii for the H and the neutral Cl atoms (2.95 Å) [10b,12c]. The observed short C–H···Cl distance in **4** (2.414 Å) implies a strong imidazole C(4)–H···Cl hydrogen-bonding interaction.

Table 4
Hydrogen-bonding (C/N–H···Cl/N) parameters for $[(\eta^6\text{-}C_6H_6)Ru(L^2)\text{-}Cl]^+$ in (**1**), $[(\eta^6\text{-}C_6H_6)Ru(HL^3)Cl]^+$ in (**2**), $[(\eta^6\text{-}C_6H_6)Ru(L^4)Cl]^+$ in (**3**), $[(\eta^6\text{-}C_6H_6)Ru(HL^5)Cl]^+$ in (**4**)

D–H···A	H···A (Å)	D···A (Å)	D–H···A
$[(\eta^6\text{-}C_6H_6)Ru(L^2)Cl]^+$ unit in ***1***			
C4–H4···Cl1	2.588	3.4572(10)	137.2°[i]
C6–H6···Cl2	2.712	3.7030(9)	152.8°[i]
$[(\eta^6\text{-}C_6H_6)Ru(HL^3)Cl]^+$ unit in ***2***			
N2–H1N···Cl	2.231[ii]	3.1747(8)[ii]	155.0°[ii]
C9–H9···Cl	2.715[iii]	3.4881(7)[iii]	127.9°[iii]
$[(\eta^6\text{-}C_6H_6)Ru(L^4)Cl]^+$ unit in ***3***			
C7–H7···Cl	2.731[iv]	3.7773(13)[iv]	162.2°[iv]
C14–H14···Cl	2.718[v]	3.6805(13)[v]	147.7°[v]
$[(\eta^6\text{-}C_6H_6)Ru(HL^5)Cl]^+$ unit in ***4***			
N2–H1N···Cl	2.244[vi]	3.2053(7)[vi]	158.5°[vi]
C13–H13···Cl	2.414[vii]	3.4534(19)[vii]	169.2°[viii]

[i] $2-x, 1-y, -z$.
[ii] $2-x, -y, 1-z$.
[iii] $x, 0.5-y, 0$.
[iv] $1-x, -y, 2-z$.
[v] $1-x, -y, 1-z$.
[vi] $-x, -y, 2-z$.
[vii] $1+x, y, z$.
[viii] $-1+x, y, z$.

3.4.1. *$[(\eta^6\text{-}C_6H_6)Ru(L^2)Cl][PF_6]$ (**1**) and $[(\eta^6\text{-}C_6H_6)\text{-}Ru(HL^3)Cl][PF_6]$ (**2**)*

In **1**, two intermolecular C–H···Cl hydrogen bonding interactions [5a,6k,10–14] linking two neighboring molecules: (i) the Ru-coordinated Cl^- ion Cl(1) and C–H(4) of C_6H_6 ring; and (ii) the organic chlorine atom Cl(2) present in *p*-chlorophenyl group of L^2 and C–H(6) of C_6H_6 ring are present. Such an interaction leads to the formation of a discrete dimeric unit (Fig. S5, Supplementary material).

In **2**, intermolecular N–H···Cl contacts [26] between Ru-coordinated Cl^- ion and N–H of pyrazole are present. This is an example of self-complementary hydrogen-bonding interaction (Fig. 3) [14a]. The dimeric units in turn are involved in C–H···Cl contacts with molecules in the same layer via C–H of pyridyl and Ru-coordinated Cl^- ion, resulting in the formation of a one-dimensional hydrogen-bonded chain (Fig. 3). Non-covalent interactions involving metal-bound HL^3 has been reported recently [27].

3.4.2. *$[(\eta^6\text{-}C_6H_6)Ru(L^4)Cl][PF_6]$ (**3**)*

Intermolecular C–H···Cl contacts between Ru-coordinated Cl^- ion and C–H of both pyridine and pyrazole rings are present. The C–H···Cl interaction involving C–H of pyrazole and Ru-coordinated Cl^- ion leads to the formation of dimeric motifs, via self-complementary hydrogen-bonding interactions. Such dimeric units are involved in additional C–H···Cl contacts with molecules in the same layer via C–H of pyridyl and the Cl^- ion, affording tetrameric units (Fig. 4(a)). In essence, Ru-coordinated Cl^- ion is engaged in bifurcated hydrogen-bonding interactions [12b,13a,14], leading to the formation of a one-dimensional hydrogen-bonded chain (Fig. 4(a)). These one-dimensional chains are involved in two types of π–π interactions [28]. One such interaction is involving coordinated C_6H_6 rings of neighbouring molecules of adjacent chains (Fig. 4(b)). The centroid–centroid distance between the two benzene rings is 3.732 Å, with a perpendicular distance between the rings of 3.289 Å and displacement angle (measured by the angle between the benzene ring normal and the centroid-centroid vector), the dihedral angle between the planes is 0.0° (dihedral angle for ideal stacked geometry = 0°), $\beta = 28.21°$, indicating strong parallel displaced π–π stacking interaction between the rings [28–30]. The other one is involving phenyl rings of benzyl groups of neighboring molecules of adjacent chains (Fig. 4(b)). The centroid–centroid distance between the two phenyl rings is 3.685 Å, with a perpendicular distance between the rings of 3.230 Å, the

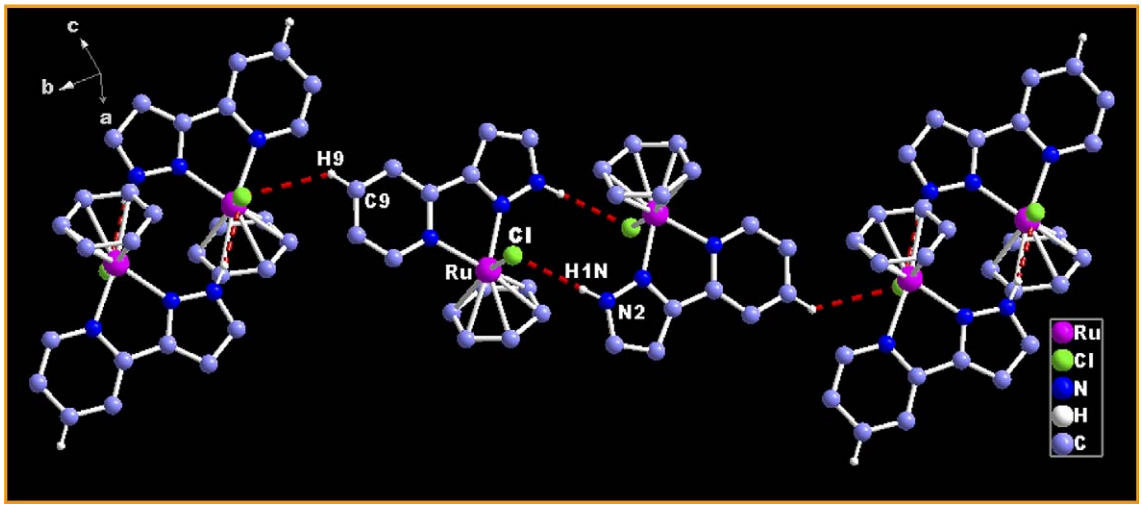

Fig. 3. View of the formation of the dimer and 1-D chain through C–H···Cl hydrogen bonding in $[(\eta^6\text{-}C_6H_6)Ru(HL^3)Cl]^+$ unit in **2**. All the hydrogen atoms except those involved in hydrogen bonding have been omitted for clarity.

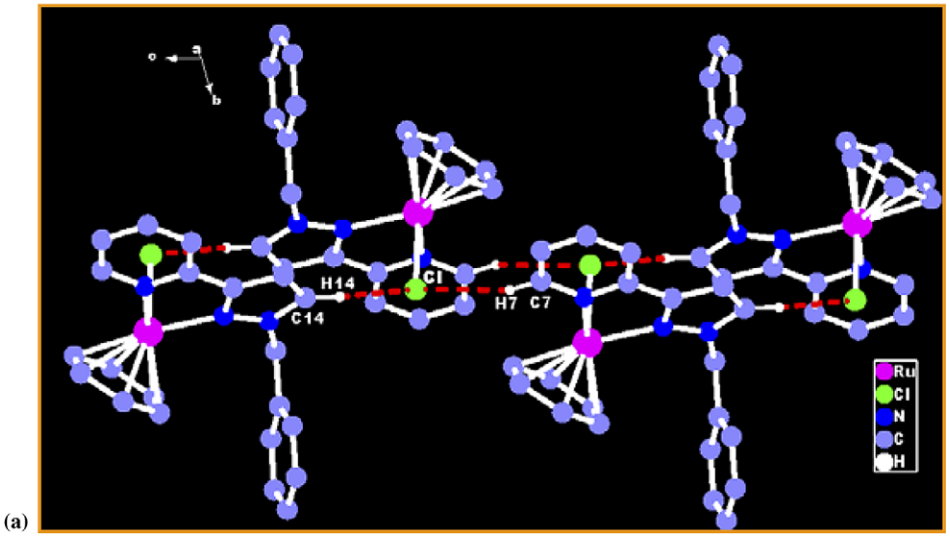

(a)

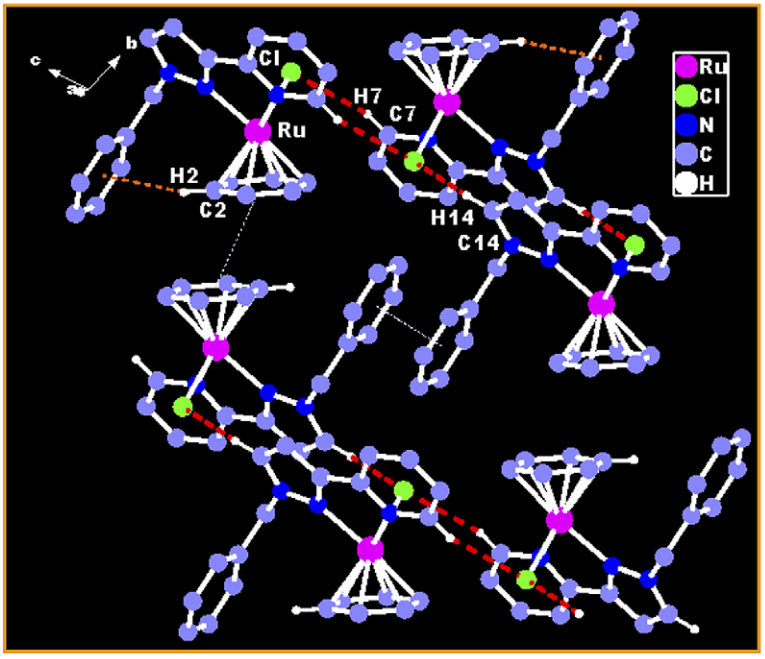

(b)

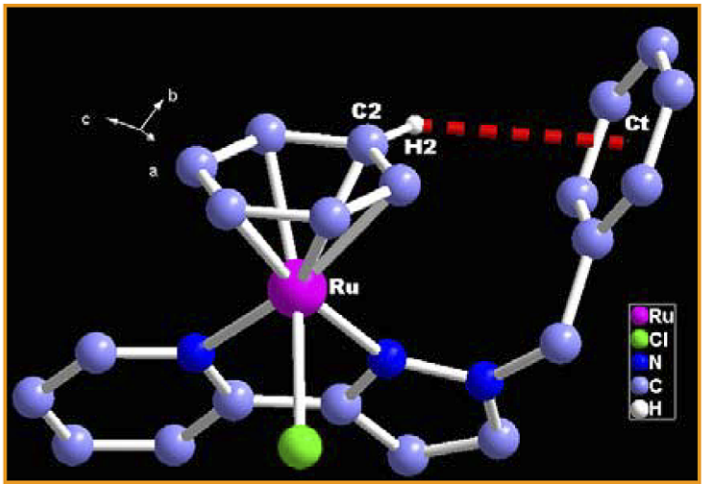

(c)

Fig. 4. (a) A perspective view of the formation of a tetramer through C–H···Cl hydrogen bonding of $[(\eta^6\text{-}C_6H_6)Ru(L^4)(Cl)]^+$ unit in **3**. (b) A view of the dimerization of tetramer through π–π stacking of: (i) phenyl (L^4)-phenyl (L^4); and (ii) $(\eta^6\text{-}C_6H_6)Ru$–$(\eta^6\text{-}C_6H_6)Ru$. (c) A view of C–H···π interaction involving C_6H_6 ring with the dangling phenyl arm of L^4. All the hydrogen atoms except those involved in hydrogen bonding have been omitted for clarity.

dihedral angle between the planes is 0.0° and displacement angle, $\beta = 28.78°$, indicating strong parallel displaced π–π stacking interaction between the rings [28–30]. These π–π stacking interactions eventually lead to the formation of a two-dimensional network (Fig. 5). In addition to aforementioned intermolecular interactions, **3** is engaged in intramolecular C–H···π interactions [8a,29,30] involving C–H of C_6H_6 with the dangling phenyl ring of benzyl group of L^4 [C2–H2···Ct (phenyl ring centroid) distance: 2.798 Å; C2···Ct distance: 3.641 Å; C–H···C_t angle, $\theta = 134°$ (Fig. 4(c)) [8a,28–30].

3.4.3. $[(\eta^6\text{-}C_6H_6)Ru(HL^5)Cl][PF_6]$ (**4**)

The packing diagram of **4** reveals intermolecular C–H···Cl contacts between Ru-coordinated Cl^- ion and C–H of imidazole ring and additional N–H···Cl contacts [26] with a neighboring dimer in the same layer generating tetrameric units (Fig. 6(a)). To our knowledge, this is the first time that such tetrameric units have been identified, solely via a combination of C–H···Cl and N–H···Cl hydrogen-bonding interactions. (ii) Parallel displaced π–π stacking interaction between the pyridyl/imidazolyl rings of HL^5 (Fig. 6(b)) (centroid–centroid distance: 3.876 Å; perpendicular distance between two pyridyl-imidazolyl planes: 3.243 Å; the dihedral angle between the planes is 0.0°; displacement angle, $\beta = 33.19°$) have also been realized [28–30].

3.4.4. Rationalization of observed non-covalent interactions

In the present group of organometallic molecules, there are four distinct types of C–H···Cl interactions between the metal-bound chloride ion (acceptors) and the C–H (donors) on the same or an adjacent molecule (vide supra). The identified donors are the C–H of coordinated C_6H_6, the H^4 or H^6 atom of a pyridine ring, the H^5 atom of a pyrazole ring, and the NH groups of non-coordinated nitrogens of pyrazole and imidazole. Careful analysis of the non-covalent interactions/supramolecular architectures noticed here (Figs. 3, 4, 6, and Fig. S5), along with the above observations, led us to present the following hypotheses. (1) From the point of view of charge density on the coordinated benzene rings, which is tuned by the extent of donation of electron density to the Ru(II) ion, the rings are deactivated. This will cause the C–H groups ideally suited to take part in C–H···Cl hydrogen bonding interactions. This has been observed in this work. (2) Considering charge distribution in the pyridine ring(s) present in ligands L^2, HL^3, L^4, and HL^5, which is tuned by the withdrawal of electrons from the ring-carbon atoms towards the nitrogen atom, and donation of electron density to the metal ion, the rings are deactivated. This will cause the positions 4 and 6 to be electron-deficient, and the C–H groups would thereby be ideally suited to take part in C–H···Cl hydrogen bonding interactions [14a]. This has been identified in this work. 3) For pyrazole groups present in L^2, HL^3, and L^4 the electron-deficient sites are 3- and

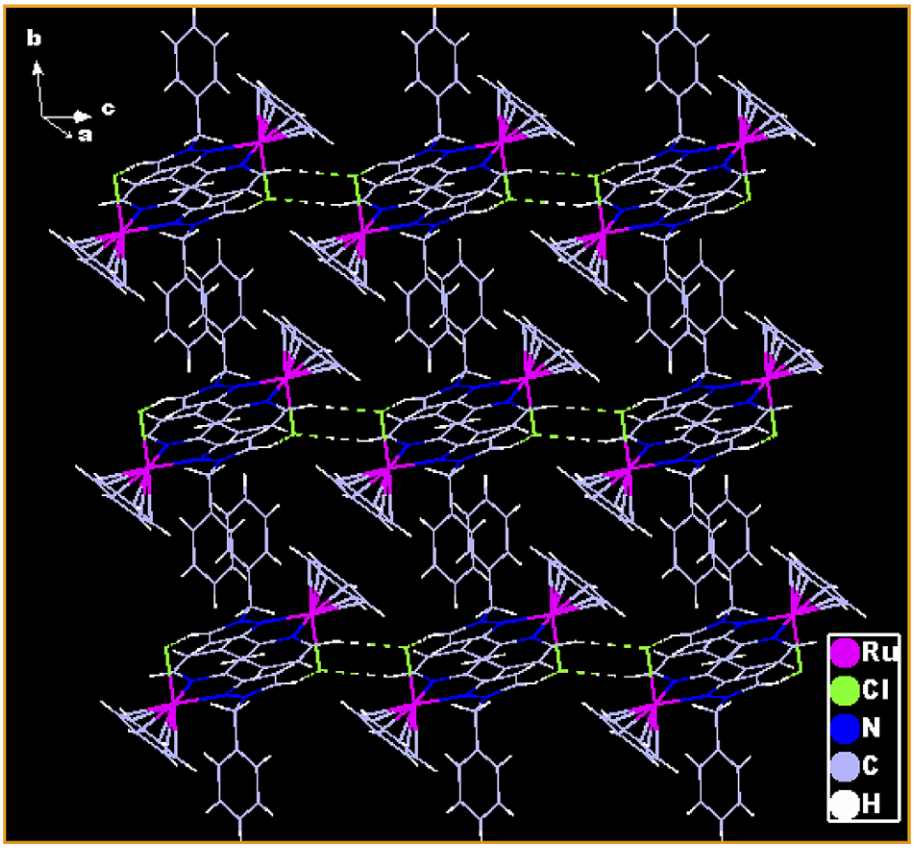

Fig. 5. Three horizontal chains of $[(\eta^6\text{-}C_6H_6)Ru(L^4)(Cl)]^+$ unit in **3** formed by C–H···Cl hydrogen-bonding interactions; three vertical chains are formed by π–π stacking of phenyl groups of L^4.

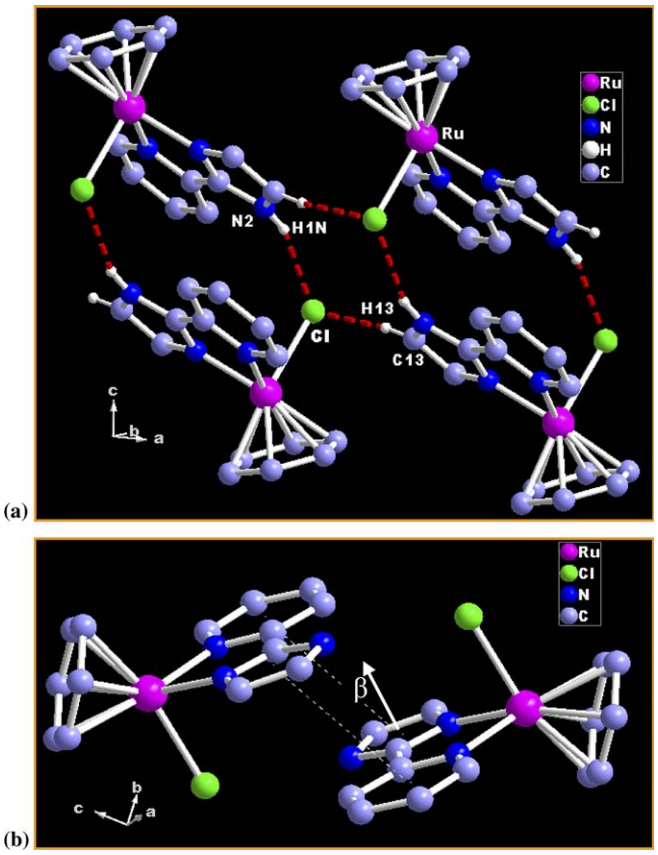

Fig. 6. (a) View of the tetramer formed via C–H···Cl and N–H···Cl hydrogen-bonding of $[(\eta^6\text{-}C_6H_6)Ru(HL^5)Cl]^+$ unit in **4**. (b) View of the dimer of $[(\eta^6\text{-}C_6H_6)Ru(HL^5)Cl]^+$ unit in **4**, pyridyl-imidazole/π–π stacking. All the hydrogen atoms except those involved in hydrogen bonding have been omitted for clarity.

5-positions [14a]. Therefore, involvement of pyrazole 5H proton in C–H···Cl hydrogen bonding interaction observed here justifies our hypothesis. (4) The pyrazole NH and imidazole NH protons in coordinated HL^3 and HL^5 are expected to be acidic and therefore be ideally suited to participate in N–H···Cl hydrogen bonding interactions. In fact, such an expectation has been realized here. (5) We believe that the C–H···π and π–π stacking interactions observed here are due to the flexible benzyl group present in the ligand L^4.

The only structurally characterized closely similar complex from the corresponding 2,2′-bipyridine (bipy) family is $[(\eta^6\text{-}C_6H_6)Ru(bipy)(MeCN)][CF_3SO_3]_2$ [6l]. Understandably, this complex is not capable of showing C–H···Cl interactions. We examined the X-ray structure of $[(\eta^6\text{-}C_6H_6)Ru(bipy)(CH_3CN)][CF_3SO_3]_2$ [6l] but no other intermolecular non-covalent interactions are found. Examination of the X-ray structure of $[(\eta^6 - p\text{-}MeC_6H_4\text{-}CHMe_2)Ru(pyz)_2Cl][PF_6]$ (pyz = pyrazine) [25a] however reveals weak (H···Cl: 2.9423 Å; C–H···Cl: 129.77°) C–H···Cl interactions (Fig. S6, Supplementary material). We are inclined to believe that the presence of both a five-membered and a six-membered hetrocyclic rings in the chosen ligands has contributed to the observation of noteworthy non-covalent interactions.

4. Conclusions

Despite several examples of structurally characterized mononuclear three-legged half-sandwich complexes of type $\{(\eta^6\text{-}C_6H_6)Ru(L)Cl\}^+$ (L = neutral bidentate heterocyclic N-donor hybrid ligands), few systematic studies have been made to design this class of half-sandwich complexes with the critical roles that the ancillary ligands play in fine-tuning structure-bonding properties of these organometallic molecules. In this work particular attention has been placed to bidentate N-donor ligands with two different heterocyclic rings. The ligands used in this work carry sites suitable for linking molecules preferentially through non-covalent interactions. In the course of the studies on these piano-stool complexes we were able to discover that Ru-coordinated benzene rings and the bidentate ligands chosen here had a pronounced tendency to participate in non-covalent interactions (C–H···Cl, N–H···Cl, C–H···π and π–π) in the solid state. The present study thus provides further information pertinent to a better understanding of the non-covalent interactions in the structure directing organometallic units $[(\eta^6\text{-}C_6H_6)Ru(L)Cl]^+$.

Acknowledgements

This work is supported by grants from the Department of Science and Technology, Government of India and the Council of Scientific and Industrial Research, New Delhi. H.M. gratefully acknowledges University Grants Commission (UGC), New Delhi for a Junior Research Fellowship. We thank Vibha Mishra for the synthesis of HL^5. R.M. gratefully acknowledges the award of a joint collaborative grant with Prof. Siegfried Schindler funded by the Volkswagen Foundation, Germany and the donation of a HP 8453 diode-array spectrophotometer. Comments of the reviewers at the revision stage are highly appreciated.

Appendix A. Supplementary material

Crystallographic data for the structures included in this paper have been deposited with the Cambridge Crystallographic Data Centre as Supplementary Publication No. CCDC reference numbers 290119 (**1**), 290120 (**2**), 290121 (**3**), and 290122 (**4**). Copies of the data can be obtained free of charge on application to CCDC, 12 Union Road, Cambridge, CB2 1EZ, UK, fax: +44 1223 336 033, e-mail: deposit@ccdc.cam.ac.uk, www: http://www.ccdc.cam.ac.uk. Supplementary data associated with this article can be found, in the online version, at doi:10.1016/j.jorganchem.2006.04.037.

References

[1] (a) H. Le Bozec, D. Touchard, P.H. Dixneuf, Adv. Organomet. Chem. 29 (1989) 163;
(b) M.A. Bennett, Coord. Chem. Rev. 166 (1997) 225.
[2] (a) R. Noyori, S. Hashiguchi, Acc. Chem. Res. 30 (1997) 97;
(b) T. Naota, H. Takaya, S.-I. Murahashi, Chem. Rev. 98 (1998) 2599;

(c) M.J. Palmer, M. Wills, Tetrahedron: Asym. 10 (1999) 2045;
(d) D. Carmona, M.P. Lamata, L.A. Oro, Eur. J. Inorg. Chem. (2002) 2239.

[3] (a) I. Moldes, J. de la Encarnación, J. Ros, Á. Alvarez-Larena, J.F. Piniella, J. Organomet. Chem. 566 (1998) 165;
(b) F. Simal, A. Demonceau, A.F. Noels, Tetrahedron Lett. 39 (1998) 3493;
(c) J.W. Faller, B.J. Grimmond, Organometallics 20 (2001) 2454;
(d) R.K. Rath, M. Nethaji, A.R. Chakravarty, Polyhedron 20 (2001) 2735;
(e) D.L. Davies, J. Fawcett, S.A. Garratt, D.R. Russell, Organometallics 20 (2001) 3029;
(f) J. Soleimannejad, A. Sisson, C. White, Inorg. Chim. Acta 352 (2003) 121;
(g) H. Brunner, T. Zwack, M. Zabel, W. Beck, A. Böhm, Organometallics 22 (2003) 1741;
(h) S.B. Wendicke, E. Burri, R. Scopelliti, K. Severin, Organometallics 22 (2003) 1894;
(i) V. Cadierno, J. Díez, J. García-Álvarez, J. Gimeno, Organometallics 23 (2004) 3425;
(j) J.R. Berenguer, M. Bernechea, J. Forniés, A. García, E. Lalinde, Organometallics 23 (2004) 4288;
(k) C. Daguenet, R. Scopelliti, P.J. Dyson, Organometallics 23 (2004) 4849;
(l) T.J. Geldbach, P.J. Dyson, J. Am. Chem. Soc. 126 (2004) 8114, references therein.

[4] Y.K. Yan, M. Melchart, A. Habtemariam, P.J. Sadler, Chem. Commun. (2005) 4764.

[5] (a) R. Fernandez, M. Melchart, A. Habtemariam, S. Parsons, P.J. Sadler, Chem. Eur. J. 10 (2004) 5173;
(b) H. Chen, J.A. Parkinson, S. Parsons, R.A. Coxall, R.O. Gould, P.J. Sadler, J. Am. Chem. Soc. 124 (2002) 3064.

[6] (a) R.J. Restivo, G. Ferguson, D.J. O'Sullivan, F.J. Lalor, Inorg. Chem. 14 (1975) 3046;
(b) M. Stebler-Röthlisberger, W. Hummel, P.A. Pittet, H.-B. Bürgi, A. Ludi, A.E. Merbach, Inorg. Chem. 27 (1988) 1358;
(c) W.S. Sheldrick, S. Heeb, J. Organomet. Chem. 377 (1989) 357;
(d) W.S. Sheldrick, S. Heeb, Inorg. Chim. Acta 168 (1990) 93;
(e) W. Luginbühl, P. Zbinden, P.A. Pittet, T. Armbruster, H.-B. Bürgi, A.E. Merbach, A. Ludi, Inorg. Chem. 30 (1991) 2350;
(f) F.B. McCormick, D.D. Cox, W.B. Gleason, Organometallics 12 (1993) 610;
(g) L.R. Hanton, T. Kemmitt, Inorg. Chem. 32 (1993) 3648;
(h) H. Asano, K. Katayama, H. Kurosawa, Inorg. Chem. 35 (1996) 5760;
(i) S. Bhambri, D.A. Tocher, J. Chem. Soc., Dalton Trans. (1997) 3367;
(j) H. Kurosawa, H. Asano, Y. Miyaki, Inorg. Chim. Acta 270 (1998) 87;
(k) J.G. Małecki, J.O. Dziegielewski, M. Jaworska, R. Kruszynski, T.J. Bartczak, Polyhedron 23 (2004) 885;
(l) W. Lackner, C.M. Standfest-Hauser, K. Mereiter, R. Schmid, K. Kirchner, Inorg. Chim. Acta 357 (2004) 2721.

[7] (a) Z. Shirin, R. Mukherjee, J.F. Richardson, R.M. Buchanan, J. Chem. Soc., Dalton Trans. (1994) 465;
(b) Z. Shirin, A. Pramanik, P. Ghosh, R. Mukherjee, Inorg. Chem. 35 (1996) 3431.

[8] (a) D. Braga, F. Grepioni, E. Tedesco, Organometallics 17 (1998) 2669;
(b) D. Braga, L. Maini, M. Polito, E. Tagliavini, F. Grepioni, Coord. Chem. Rev. 246 (2003) 53.

[9] L. Brammer, J.C.M. Rivas, R. Atencio, S. Fang, F.C. Pigge, J. Chem. Soc., Dalton Trans. (2000) 3855.

[10] (a) R. Taylor, O. Kennard, J. Am. Chem. Soc. 104 (1982) 5063;
(b) G. Aullón, D. Bellamy, L. Brammer, E.A. Bruton, A.G. Orpen, Chem. Commun. (1998) 653;
(c) C. Janiak, T.G. Scharmann, Polyhedron 22 (2003) 1123.

[11] (a) D. Braga, S.M. Draper, E. Champeil, F. Grepioni, J. Organomet. Chem. 573 (1999) 73;
(b) A. Singh, M. Chandra, A.N. Sahay, D.S. Pandey, K.K. Pandey, S.M. Mobin, M.C. Puerta, P. Valerga, J. Organomet. Chem. 689 (2004) 1821;
(c) S.K. Singh, M. Chandra, D.S. Pandey, M.C. Puerta, P. Valerga, J. Organomet. Chem. 689 (2004) 3612;
(d) S.K. Singh, M. Trivedi, M. Chandra, A.N. Sahay, D.S. Pandey, Inorg. Chem. 43 (2004) 8600.

[12] (a) L. Brammer, Chem. Soc. Rev. 33 (2004) 476;
(b) L. Brammer, in: G.R. Desiraju (Ed.), Perspectives in Supramolecular Chemistry–Crystal Design: Structure and Function, vol. 7, Wiley, Chichester, 2003, pp. 1–75;
(c) T. Steiner, Angew. Chem., Int. Ed. 41 (2002) 48;
(d) L. Brammer, E.A. Bruton, P. Sherwood, Cryst. Growth Des. 1 (2001) 277;
(e) P.K. Thallapally, A. Nangia, CrystEngComm 27 (2001) 1;
(f) C.B. Aakeröy, T.A. Evans, K.R. Seddon, I. Pálinkó, New J. Chem. (1999) 145.

[13] (a) R. Kapoor, A. Kataria, P. Kapoor, P. Venugopalan, Trans. Met. Chem. 29 (2004) 425;
(b) M. Prabhakar, P.S. Zacharias, S. Das, Inorg. Chem. 44 (2005) 2585.

[14] (a) V. Balamurugan, M.S. Hundal, R. Mukherjee, Chem. Eur. J. 10 (2004) 1683;
(b) V. Balamurugan, W. Jacob, J. Mukherjee, R. Mukherjee, CrystEngComm 6 (2004) 396;
(c) V. Balamurugan, R. Mukherjee, CrystEngComm 7 (2005) 337.

[15] A.J. Amoroso, A.M.C. Thompson, J.C. Jeffery, P.L. Jones, J.A. McCleverty, M.D. Ward, J. Chem. Soc., Chem. Commun. (1994) 2751.

[16] J. Mukherjee, R. Mukherjee, Dalton Trans. (2006) 1611.

[17] B. Chiswell, F. Lions, B. Morris, Inorg. Chem. 3 (1964) 110.

[18] R.A. Zelonka, M.C. Baird, Can. J. Chem. 50 (1972) 3063.

[19] W.J. Geary, Coord. Chem. Rev. 7 (1971) 81.

[20] L.J. Farrugia, WINGX ver 1.64, An Integrated Systems of Windows Programs for the SolutionRefinement and Analysis of Single-crystal X-ray Diffraction Data, Department of Chemistry, University of Glasgow, 2003.

[21] DIAMOND Ver 2.1c, Crystal Impact GbR, Bonn, Germany, 1999.

[22] R. Mukherjee, Coord. Chem. Rev. 203 (2000) 151.

[23] T.K. Lal, R. Mukherjee, Polyhedron 16 (1997) 3577.

[24] P.L. Jones, J.C. Jeffery, J.A. McCleverty, M.D. Ward, Polyhedron 16 (1997) 1567.

[25] (a) D.A. Tocher, R.O. Gould, T.A. Stephenson, M.A. Bennett, J.P. Ennett, T.W. Matheson, L. Sawyer, V.K. Shah, J. Chem. Soc., Dalton Trans. (1983) 1571;
(b) A. Frodl, D. Herebian, W.S. Sheldrick, J. Chem. Soc., Dalton Trans. (2002) 3664;
(c) T. Hayashida, H. Nagashima, Organometallics 21 (2002) 3884;
(d) L. Lalrempuia, K.M. Rao, Polyhedron 22 (2003) 3155.

[26] (a) J.C.M. Rivas, R. Prabaharan, R.T.M. De Rosales, L. Metteau, S. Parsons, Dalton Trans. (2004) 2800;
(b) K.W. Törnroos, D. Chernyshov, M. Hostettler, H.-B. Bürgi, Acta Crystallogr., Sect. C 61 (2005) m450.

[27] R.-Q. Zou, X.-H. Bu, M. Du, Y.-X. Sui, J. Mol. Struct. 707 (2004) 11.

[28] C. Janiak, J. Chem. Soc., Dalton Trans. (2000) 3885.

[29] (a) D.L. Reger, J.R. Gardinier, R.F. Semeniuc, M.D. Smith, Dalton Trans. (2003) 1712;
(b) D.L. Reger, R.F. Semeniuc, M.D. Smith, Cryst. Growth Des. 5 (2005) 1181.

[30] G. Agrifoglio, A.R. Karam, E.L. Catarí, T. González, R. Atencio, Acta Crystallogr., Sect. E 61 (2005) o2613.